地震研究所彙報
Bull. Earthq. Res. Inst.
Univ. Tokyo
Vol. 83 (2008) pp. 273-279

The Effects of Negative Stress Drop on Fault Rupture —The 2004 mid-Niigata (Chuetsu), Japan, earthquake

Takashi Miyatake*, Aitaro Kato, Kazuhito Hikima and Takeshi Kimura

Earthquake Research Institute, University of Tokyo

Abstract

We investigate spatiotemporal distribution in a kinematic slip model of the 2004 mid-Niigata (Chuetsu) earthquake, focusing on the relationship between rupture time and stress drop. Stress drop distribution is calculated from the final slip distribution inferred from waveform inversion. There are negative stress drop regions near the edges of inferred asperities. Rupture delays were detected in the mean slip rate time functions. Combining the above distribution, we found delayed rupture within regions of negative stress drop. In these negative stress drop regions, rupture propagation is expected to arrest because a positive stress drop promotes rupture. It should be emphasized that our results were obtained without reconstructing the dynamic faulting process.

Key words: Rupture Process, The 2004 mid-Niigata earthquake, Stress drop

1. Introduction

The faulting process, i.e., space-time distributions of fault slips of past earthquakes, have been estimated by many seismologists (*e.g.,* Liu, *et al.,* 2006, Liu and Archuleta, 2004; Wald and Heaton, 1994; Yagi, 2004). In addition to these kinematic fault models, dynamic models of earthquakes have also been constructed with the constraints of the kinematic parameters (*e.g.,* Quin, 1990; Miyatake, 1992ab; Mikumo and Miyatake, 1998; Miyatake *et al.,* 2004; Olsen *et al.* 1997; Peyrat *et al.,* 2001). Knowledge of dynamic parameters is important not only to understand earthquake source physics, but also strong ground motion simulations, which require realistic source models for probabilistic modeling (Irikura *et al.,* 2004). However, the dynamic model depends on the kinematic model selected. Several different kinematic models often exist for a single earthquake, each obtained with a different inversion method, waveform data set, or modeling of kinematic source.

Depending on numerous additional factors including computational method and computational parameters adopted, dynamic models based on kinematic models are also not unique. As one example of the additional complexity of dynamic models, Guatteri and Spudich (2000) demonstrated that two key dynamic parameters, Dc and peak stress, cannot be uniquely estimated from band-limited waveforms.

In this manuscript, we study the details of the kinematic model of the 2004 mid-Niigata (Chuetsu) earthquake, which occurred within a dense network of seismographs (Fig. 1), and obtained important information on physical faulting process of the event without reconstructing a sophisticated dynamic model.

2. The 2004 mid-Niigata earthquake

The 2004 mid-Niigata earthquake of M_w 6.6 occurred in the back-arc area of the main Japanese island as a shallow inland dip-slip earthquake. The source region was located in the eastern margin of a thick sedimentary basin (Kato *et al.* 2006). It caused serious damage in and around the source region. The main shock was followed by significant aftershock activity, and the number of large aftershocks was significantly greater than those associated with other recent inland earthquakes in Japan.

Kinematic model of the 2004 mid-Niigata earthquake

Several inversion studies have been performed on the 2004 mid-Niigata earthquake, each of which has

* e-mail: miyatake@eri.u-tokyo.ac.jp (1-1-1, Yayoi, Bunkyo-ku, Tokyo 113-0032, Japan)

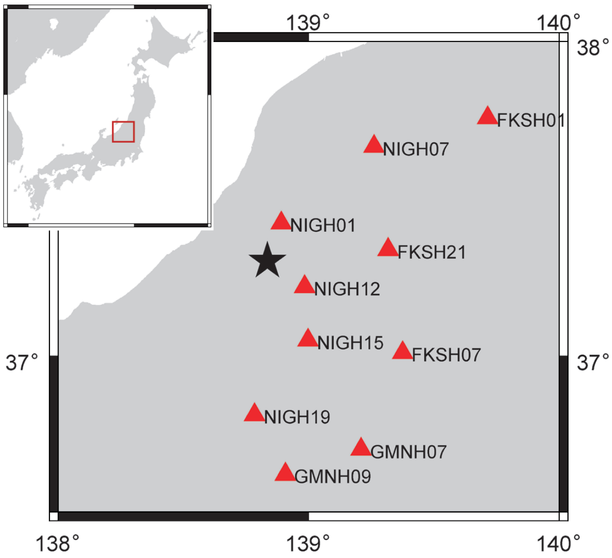

Fig. 1. Hypocenter of the 2004 Chuetsu earthquake is plotted as a black star. Red triangles represent KiK-net stations that recorded data compared to synthetic seismograms (see also Fig. 5).

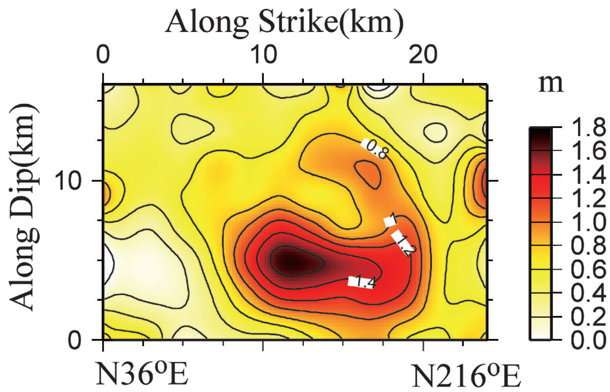

Fig. 2. Slip distribution inferred from waveform inversion results obtained by Hikima and Koketsu (2005).

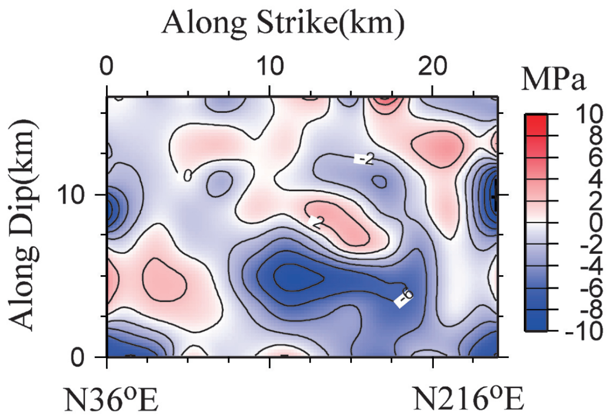

Fig. 3. Static stress change distribution calculated using Okada's (1992) Green's functions.

yielded slightly different results (*e.g.,* Hikima and Koketsu, 2005; Honda *et al.,* 2005; Asano and Iwata, 2009). In general, the waveform inversion results differ because of specific choices made regarding, for instance, the inclusion of geodetic data or teleseismic data, the inversion algorithm itself, and different Green's functions (*e.g.* 1D, hybrid 1D, or 3D). The above three studies did not use geodetic nor teleseismic data, but used near-field ground motion records, although number of waveforms are different. On the other hand, the Green's functions or the structure models for the functions differed. This earthquake occurred along a structural boundary between low seismic velocity sediments in a hanging wall and basement rocks in the footwall (Kato *et al.* 2006). The source region is structurally heterogeneous, and many of the differences among the results of the three groups listed above may stem from differences in the Green's functions used for inversion. Therefore, a well-calibrated Green's function is indispensable for building a precise kinematic model (Graves and Wald, 2001).

We chose to use the results obtained by Hikima and Koketsu (2005) because: 1) they estimated hybrid 1D structures for each station via inversion of the waveforms of aftershocks to calculate accurate Green's functions, and 2) the propagation speed of the time windows used in their inversion is 2.9 km/s, which is fast enough coupled with the relatively long time window (8 sec) to estimate rupture delay times. In their approach, rupture time is not an estimated parameter. Instead, the amplitudes of subfault slip rate time functions at successive time steps, which propagate at a constant speed from a starting point, are obtained. If the velocity of the moving window is greater than rupture velocity, and if the total duration of the time windows is sufficiently long, it is possible to detect a delayed rupture. The waveform inversion results obtained by Hikima and Koketsu (2005) are amenable for detecting rupture delay. Although Asano and Iwata (2007) also computed a hybrid 1D crustal structure when obtaining well-calibrated Green's functions, the time window propagation speed of 1.9 km/s is too slow to detect any

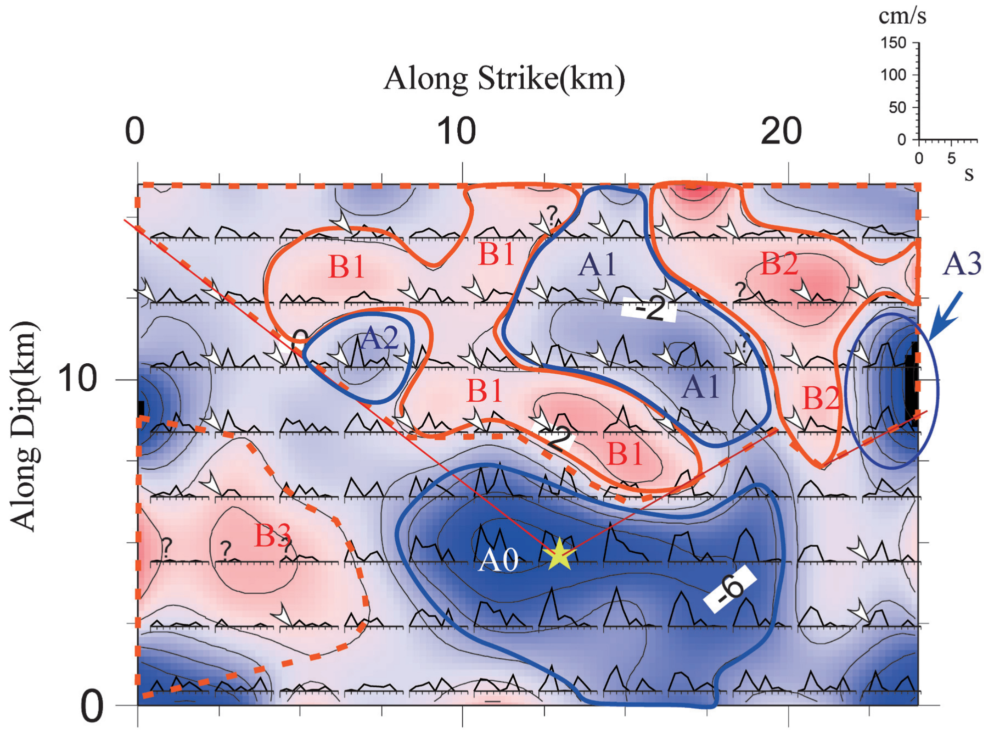

Fig. 4. Stress change distribution and mean slip rate time functions on the fault plane. Arrows indicate rupture time delays. The yellow star indicates the initial point of fault rupture. Solid orange lines demarcate negative stress drop zones. Dashed orange lines encompass zones of negative stress drop and "shadow" regions. See text for further details.

rupture delay. It is worth noting, however, that the slip distributions of Hikima and Koketsu (2005) and Asano and Iwata (2007) are very similar. Honda *et al.* (2005) used a similar inversion algorithm to that of Asano and Iwata (2007), but different crustal models. Honda *et al.* (2005) used only three separate crustal models, i.e., two velocity structure models for stations on the hanging wall and one model for footwall side stations. In contrast, Asano and Iwata (2007) and Hikima and Koketsu (2005) inferred the structure for each station separately using a genetic algorithm and waveform inversion, respectively.

Slip and stress change distribution

The kinematic slip distribution obtained by Hikima and Koketsu (2005) is illustrated in Fig. 2. It possesses a maximum slip value of 1.7 m at deeper portions of the fault. The shallower (19 km along the strike and 10 km up-dip from the bottom) of the two main asperities is narrow and has a slip of 1 m connecting the deeper asperity. Based on this slip distribution, we calculated the stress change due to the earthquake (Fig. 3) using Green's functions derived by Okada (1992). Blue color indicates stress drops and red color indicates stress rises, or negative stress drops. A maximum stress drop of about 9 MPa occurred at the deeper asperity of maximum slip, which is comparable with those for other inland Japanese earthquakes (Miyatake, 1992b), but much lower than the 100 MPa maximum stress drops obtained by Bouchon (1997) for several earthquakes in California.

Negative stress drop regions are evident in the shallower half of the fault and also on the eastern part of the fault (around 3 km along strike and 4 km from the bottom in Fig. 3, see also B3 in Fig. 4). At shallow depths, a negative stress drop (Fig. 3, see also B1 in Fig. 4) separates the positive stress drop regions A1 from A0 (Fig. 4). This negative stress drop (B1) corresponds to a slip deficit (Fig. 2). There is also a corresponding slip deficit in the kinematic model estimated by Asano and Iwata (2007) and Honda *et al.* (2004). Therefore, the inference that negative stress drops correspond to locations of slip defect seems reasonable.

Delay of rupture propagation

The moment rate (or mean slip rate) time functions of the subfaults estimated by Hikima and Koketsu (2005) are superimposed on the stress change distribution in Fig. 4. Each plot starts at the arrival time of the first time window used in the inversion process, which propagates at a speed of 2.9 km/s as noted above. Arrows indicate the delayed onset of slip at each location, i.e., rupture delay, which we measured. There are delays at many subfaults, particularly in the upper half part of the fault. Regarding the relation to stress drop, delayed ruptures are in both positive (*e.g.* A1 and A2; Fig. 4) and negative stress drop regions (i.e., B1, B2, and B3).

Accounting for rupture delays at negative stress drop regions is straightforward. Because a positive stress drop promotes rupture, a negative stress drop (such as in regions B1 and B2) would be expected to arrest or decelerate rupture propagation. On the other hand, rupture onset delays in positive stress drop regions, for example, A1 and A2, can be explained as follows: a negative stress drop at B1 will cause delays not only there but also within the asperities, A1 and A2, because the onset of rupture at those two locations is affected by any delays at B1. In other words, regions A1 and A2 are "shaded" by B1 with respect to the hypocenter (yellow star in Fig. 4), and the delays measured there on the region depend on the delay at B1. On the analogy of travel time calculation, the delays at A1 and A2 are the integration of (positive or negative) delay times along the "propagation paths".

A similar argument may be made for A3 lying within the "shadow" of the negative stress drop region B2. Another important factor controlling rupture delay may be peak stress (or fracture energy). This could account for the delays at A1 and A2 if peak stresses were high enough locally. However, given that delays within positive stress drop regions are consistently observed to occur in the "shadows" cast by negative stress drops, we consider that negative stress drops play a key role in determining the rupture onset of the earthquake.

3. Discussion

We carefully studied the stress drop and the delay of moment rate time functions on the fault of the 2004 mid-Niigata earthquake, Japan, and found that rupture delay is related to the negative stress drop on the fault. In our approach, we did not use dynamic modeling. Despite the procedure adopted, we successfully obtained physically meaningful results.

In general, negative stress drops are caused by one or more of the following factors: 1) frictional properties of the fault, 2) inappropriate or inaccurate presumed fault geometry, or 3) poor inversion resolution. In the first explanation, rate-dependent frictional properties possibly account for negative stress drops (Cochard and Madariaga, 1994). According to the rate-and state friction law, if A-B > 0, slip hardening, and therefore negative stress drop occur where A and B are parameters of the rate-and state friction law (see, *e.g.,* Scholz, 2002). Likewise, a discrepancy between the fault's true geometry and that used for modeling may generate negative stress drops (Ando, 2005), particularly if fault kinks or offsets decrease slip locally. If we calculate stress distribution on the assumption of a planar fault, a negative stress drop will be obtained, and in this case the region surrounding a fault kink or step will act as a rupture barrier (Harris and Archuleta, 1991). The third explanation for negative stress drops is poor model resolution in the source inversion process. Poor resolution causes fault slip to leak towards the periphery of the fault. This smoothing around the fault edge produces the negative stress drop. In the case of the 2004 mid-Niigata earthquake, the event occurred within a dense seismic network with several seismographs located very close to the fault, so inversion resolution is not considered likely to be a significant factor.

Kato, Miyatake, and Hirata (2007) observed that the negative stress drop region is located near an abrupt transition in sediment thickness (see Fig. 3 and Fig. 7 of Kato *et al.,* 2006), above the mainshock hypocenter. They also suggested that the ductile flow of sediments above the mainshock hypocenter might act as a soft barrier against coseismic rupture because the low-velocity sediments would not sustain high stresses. This argument implies that stresses prior to the earthquake were low. Low stress or ductile flows themselves produce a low or zero stress drop, and would easily raise the residual stress level, so cause negative stress drop when combined with the above 1) fault friction property or the above 2): kink or bend (or small bump on the fault plane) corresponding to the macroscopic assumption.

We investigated rupture delay. However, to what extent are differences in waveform produced by de-

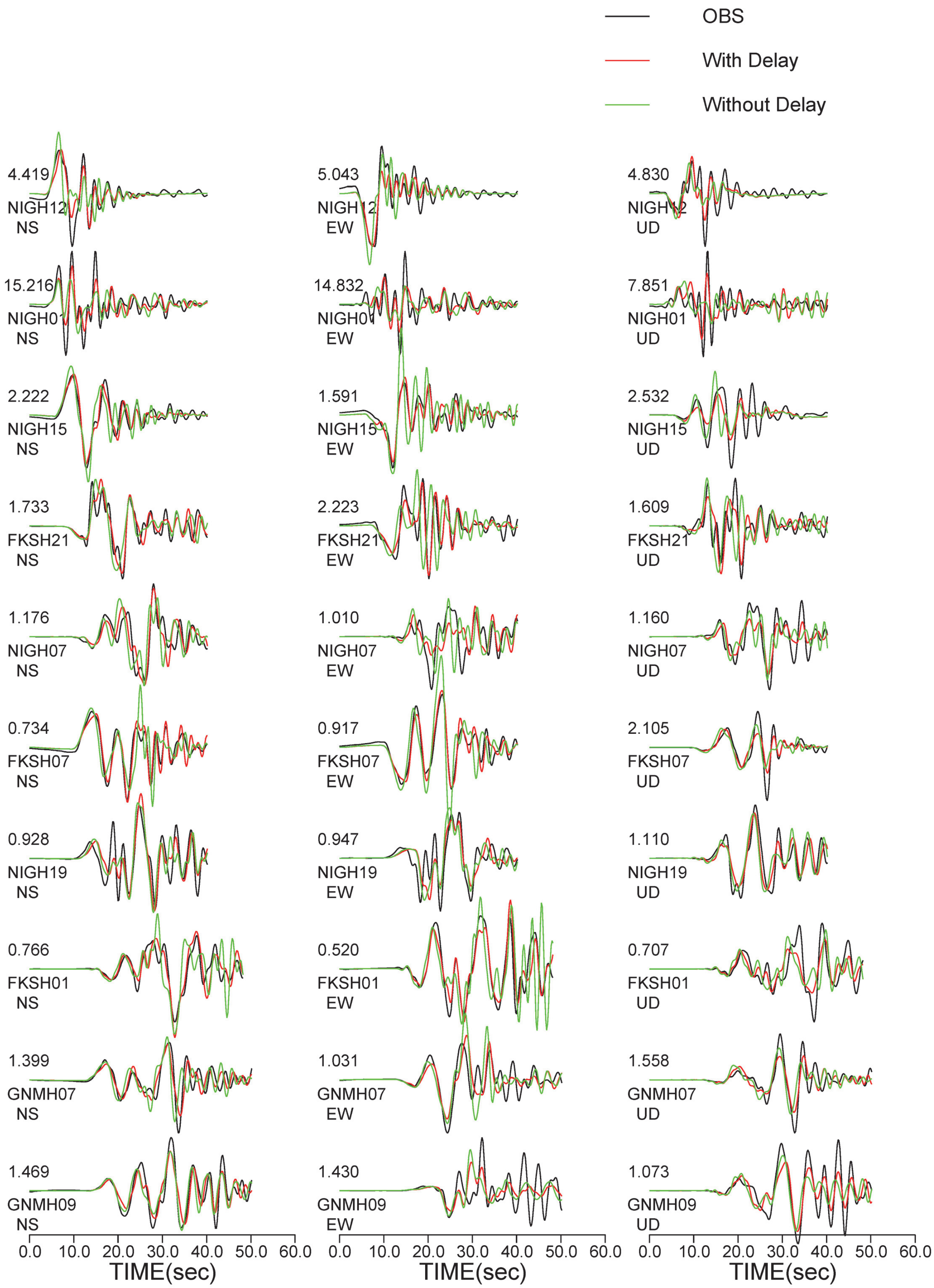

Fig. 5. Comparison between synthetic velocity waveforms from the kinematic model (Hikima and Koketsu, 2005) and those from same kinematic model without rupture delays detected in Fig. 3. Red and green lines indicate kinematic model waveforms and those without indicate rupture delays, respectively. The observed waveforms are also plotted as black lines. Numerals are peak amplitudes in cm/s.

lay time? If such a waveform change is small enough, it is impossible to detect rupture delay. Fig. 5 shows a comparison between synthetic waveforms from the original kinematic model of Hikima and Koketsu (2005) and those from the same kinematic model without rupture delays detected in Fig. 4. The kinematic model waveforms are clearly different from those without rupture delays. Waveform inversion is a complex system. It depends on many factors including differences in source modeling, data processing (low-pass or band-pass filter), and inversion technique. Besides, in the inversion using the multi-time window method, the rupture delay is not an inversion parameter. Therefore, it is difficult to calculate the resolution of the rupture delay. Instead, we demonstrated that the delays of the rupture times provide clear differences in the seismic waveforms from those without delays.

4. Conclusion

We carried out a detailed investigation of a kinematic model of the 2004 mid-Niigata earthquake and found that negative stress drops play an important role in controlling rupture propagation, particularly rupture onset delays. Because a positive stress drop promotes rupture, a negative stress drop is expected to consume elastic energy and impede rupture propagation. It is important to emphasize that these results were obtained without reconstructing the dynamic faulting process.

Acknowledgments

This research was supported in part by Special Project for Earthquake Disaster Mitigation in Urban Areas and the Grand-in-Aid for Scientific Research funding from the Ministry of Education, Culture, Sports, Science and Technology of Japan. We thank Prof. T. Yamashita for critically reading the manuscript and for his helpful suggestions.

References

Ando, R., 2005, Development of efficient spatio-temporal boundary integral equation method and theoretical study on dynamics of fault zone formation and earthquake rupture, (in Japanese, English Abstract), PhD. Thesis, University of Tokyo.

Asano, K. and T. Iwata, 2009, Source rupture process of the 2004 Chuetsu, mid Niigata prefecture, Japan, earthquake inferred from waveform inversion with dense strong motion data, *Bull. Seism. Soc. Amer.,* **99**, 123–140, doi: 10.1785/0120080257.

Bouchon, M., 1997, The state of stress on some faults of the San Andreas system as inferred from near-field strong motion data, *J. Geophys. Res.,* **102**, 11,731–11,744.

Cochard, A. and R. Madariaga, 1994, Dynamic faulting under rate-dependent friction, *PAGEOPH,* **142**, 419–445.

Graves, R.W. and D.J. Wald, 2001, Resolution analysis of finite fault source inversion using one-and three-dimensional Green's functions: 1. Strong motions, *J. Geophys. Res.,* **106** (B5), 8745–8766, 10.1029/2000JB900436.

Guatteri, M. and P. Spudich, 2000, What can strong-motion data tell us about slip-weakening fault friction laws? *Bull. Seis. Soc. Am.* **90**, 98–116.

Haris, R.A. and R.J. Archuleta, 1991, Fault steps and the dynamic rupture porcess: 2D numerical simulations of a spontaneously propagating shear fracture, *Geophys. Res. Lett.,* **18**, 893–896.

Hikima, K. and K. Koketsu, 2005, Rupture processes of the 2004 Chuetsu (mid-Niigata prefecture) earthquake, Japan: A series of events in a complex fault system, *Geophys. Res. Lett., Doi*: **10**.1029/2005GRL023588.

Honda, R., S. Aoi, N. Morikawa, H. Sekiguchi, T. Kunugi and H. Fujiwara, 2005, Ground motion and rupture process of the 2004 Mid Niigata Prefecture earthquake obtained from strong motion data of K-Net and KiK-net, *Earth Planets Space,* **57**, 527–532.

Irikura, K., H. Miyake, T. Iwata, K. Kamae, H. Kawabe and L. A. Dalguer, 2004, Recipe for predicting strong ground motions from future large earthquakes, 13th World Conference on Earthquake Engineering, Paper No. 1371.

Kato, A., S. Sakai, N. Hirata, E. Kurashimo, T. Iidaka, T. Iwasaki and T. Kanazawa, 2006, Imaging the seismic structure and stress field in the source region of the 2004 mid-Niigata prefecture earthquake: Structural zones of weakness and seismogenic stress concentration by ductile flow, *J. Geophys. Res.,* **111**, B08308, doi: 10.1029/2005JB004016.

Kato, A., T. Miyatake and N. Hirata, 2007, Effects of structural heterogeneities of fault zone on source process of the 2004 mid-Niigata Prefecture Earthquake, S143-008, Japan Geoscience Union Meeting.

Liu, P. and R.J. Archuleta, 2004, A new nonlinear finite fault inversion with three-dimensional Green's functions: Application to the 1989 Loma Prieta, California, earthquake, *J. Geophys. Res.,* **109**, B02318, doi: 10.1029/2003JB002625.

Liu, P., S. Custódio and R. J. Archuleta, 2006, Kinematic Inversion of the 2004 M 6.0 Parkfield Earthquake Including an Approximation to Site Effects, *Bull. Seismol. Soc. Am.,* **96**, S143–S158.

Mikumo, T. and T. Miyatake, 1995, Heterogeneous distribution of dynamic stress drop and relative fault strength recovered from the results of waveform inversion: The 1984 Morgan Hill California earthquake, *Bull. Seism. Soc. Amer,* **85**, 178–193.

Miyatake, T., 1992a, Dynamic rupture processes of inland earthquakes in Japan —Weak and Strong asperities, *Geophysical Research Letters,* **19**, 1041–1044.

Miyatake, T., 1992b, Reconstruction of dynamic rupture process of an earthquake with constraints of kinematic parameters, *Geophysical Research Letters,* **19**, 349–352.

Miyatake, T., Y. Yagi. and T. Yasuda, 2004, The dynamic rupture process of the 2001 Geiyo, *Japan, earthquake, Geophys. Res. Lett.,* **31**, L12612, doi: 10.1029/2004GL019721.

Okada, Y., 1992, Internal deformation due to shear and tensile faults in a half-space, *Bull. Seism. Soc. Amer.,* **82**, 1018–1040.

Olsen, K.B., R. Madariaga and R.J. Archuleta, 1997, Three-dimensional dynamic simulation of the 1992 Landers earthquake, *Science,* **278**, 834–838.

Peyrat, S., K. B. Olsen and R. Madariaga, 2001, Dynamic modeling of the 1992 Landers earthquake, *J. Geophys. Res.* **106**, 26,467–26,482.

Quin, H., 1990, Dynamic stress drop and rupture dynamics of the October 15, 1979 Imperial Valley, California, earthquake, *Tectonophysics,* **175**, 93–117.

Scholz, C. H., 2002, The mechanics of earthquakes and faulting, second edition, Cambridge University Press.

Wald, D. and T. H. Heaton, 1994, Spatial and Temporal Distribution of Slip for the 1992 Landers, California, Earthquake, *Bull. Seism. Soc. Am.,* **84**, 668–691.

Yagi, Y., 2004, Source rupture process of the 2003 Tokachi-oki earthquake determined by joint inversion of teleseismic body wave and strong ground motion data, *Earth Planet and Space,* **56**, 311–316, 2004.

(Received June 25, 2008)
(Accepted March 23, 2009)